

REFERENCES

1. E. S. Smotkin, A. J. Bard, A. Campion, M. A. Fox, T. Mallouk, S. E. Webber, and J. M. White, *J. Phys. Chem.*, **90**, 4606 (1986).
2. E. S. Smotkin, S. Cervera-March, A. J. Bard, A. Campion, M. A. Fox, T. Mallouk, S. E. Weber, and J. M. White, *ibid.*, **91**, 6 (1987).
3. A. Fujishima and K. Honda, *Nature (London)*, **238**, 37 (1972).
4. A. J. Bard, *Science*, **207**, 139 (1980).
5. H. Gerischer, in "Photoelectrochemistry, Photocatalysis and Photoreactors, Fundamentals and Developments," M. Schiavello, Editor, NATO ASI series, 146, 107 (1985).
6. R. Memming, in "Photoelectrochemistry, Photocatalysis and Photoreactors, Fundamentals and Developments," M. Schiavello, Editor, NATO ASI series, 146, 107 (1985).
7. A. Heller, in "Energy Resources through Photochemistry and Catalysis," M. Graetzel, Editor, p. 385, Academic Press, New York (1983).
8. F.-R. F. Fan and A. J. Bard, *J. Am. Chem. Soc.*, **102**, 3677 (1980).
9. Y. I. Kharkats, E. D. German, V. E. Kazarinov, A. G. Pshenichnikov, and Y. V. Pleskov, *Int. J. Hydrogen Energy*, **11**, 617 (1986).
10. G. Hodes, D. Cahen, J. Manassen, and M. J. David, *This Journal*, **127**, 2252 (1980).
11. G. Hodes, J. Manassen, and D. Cahen, *ibid.*, **127**, 544 (1980).
12. B. V. Tidak, W. T. Lu, and J. E. Coleman, in "Comprehensive Treatise of Electrochemistry," J. O'M. Bockris, Editor, pp. 13-33, Plenum Press, New York (1981).
13. D. A. Corrigan, *This Journal*, **134**, 377 (1987).

Electrochemical Flue Gas Desulfurization

Reactions in a Pyrosulfate-Based Electrolyte

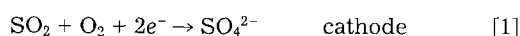
Kevin Scott,¹ Terry Fannon, and Jack Winnick*

School of Chemical Engineering, Georgia Institute of Technology, Atlanta, Georgia 30332

ABSTRACT

A new electrolyte has been found suitable for use in an electrochemical membrane cell for flue gas desulfurization (FGD). The electrolyte is primarily $K_2S_2O_7$ and K_2SO_4 , with V_2O_5 as oxidation enhancer. This electrolyte has a melting point near 300°C which is compatible with flue gas exiting the economizer of coal-burning power plants. Standard electrochemical tests have revealed high exchange current densities, around 30 mA/cm^2 , in the free electrolyte. Sulfur dioxide is found to be removed from simulated flue gas in a multiple-step process, the first of which is electrochemical reduction of pyrosulfate.

Electrochemical technology for gas separation has been used to remove trace amounts of contaminant gases and concentrate them into a by-product stream (1-4). An electrochemical driving force causes a net transfer of mass from a region of low concentration to a region of high concentration. A test cell operating on this principle has been found (5) to successfully remove and concentrate the sulfur dioxide in simulated power plant flue gas. This device utilized a ternary Li-Na-K sulfate eutectic (mp = 512°C) as the transport medium for the sulfur species. Sulfur dioxide is removed at the cathode and generated at high concentration at the anode with the net reactions



The benefits of this molten salt electrochemical flue gas desulfurization cell include: high selectivity, no waste sludge production, one-step sulfur dioxide removal and recovery, and relatively easy expansion capability by cell stacking. However, the high operating temperature ($>512^\circ\text{C}$) is incompatible with direct application to conventional power plants. The flue gases in a power plant leave the economizer at $250^\circ\text{--}400^\circ\text{C}$ (6), which is the ideal operating temperature range for the desulfurization device. A new, lower melting electrolyte must be identified. Alkali bisulfates have been studied (7), but lack sufficient thermal stability at the temperatures of interest. Here, we examine potassium pyrosulfate which is stable as a liquid in the desired temperature range. It is also widely available and inexpensive.

The commercial device would be configured like a stack of fuel cells, each with liquid electrolyte contained in a ceramic matrix. Ceramic gas-diffusion electrodes appear attractive as both cathode and anode [e.g., Ref. (8)]. At the cathode, the sulfur dioxide and oxygen present in flue gas²

must be converted into anions transportable to the anode (see Fig. 1). Here they are oxidized to sulfur trioxide and oxygen.

The process is quite similar to that in a molten carbonate fuel cell where the overall cathodic reaction is



In a sulfate electrolyte, the overall cathode reaction, Eq. [1], was found to be limited only by gas-phase diffusion of the SO_2 (9). Proper cell design can provide economic operation even at 90% SO_2 removal (5).

At the lower temperatures, with potassium pyrosulfate as electrolyte, the cathodic reactions with sulfur dioxide and oxygen must be reinvestigated. In contrast with the sulfate electrolyte, no prior study seems available. Here we examine the electrochemical behavior of molten $K_2S_2O_7$ in contact with gases containing low levels of sulfur dioxide and oxygen. The effect of V_2O_5 , a sulfur dioxide oxidation catalyst, is also explored. We focus on the cathodic processes, where the flue gas will act as oxidant, as these are expected to be rate limiting (10).

Experimental

Pyrex cell housings of various designs were employed to contain the molten electrolyte. One type is shown schematically in Fig. 2. The temperature was maintained at $340^\circ \pm 5^\circ\text{C}$ in a custom-built furnace controlled by a double-pole

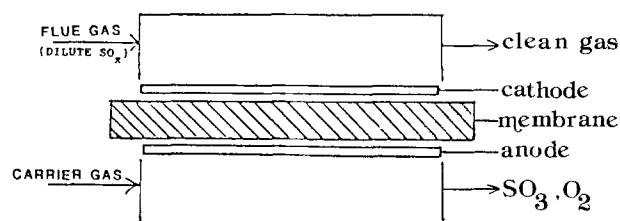


Fig. 1. Flue gas desulfurization test cell schematic

*Electrochemical Society Active Member.

¹Present address: E.I. du Pont de Nemours and Company, Wilmington, Delaware.

²Typically 0.3% SO_2 and 3-5% O_2 .

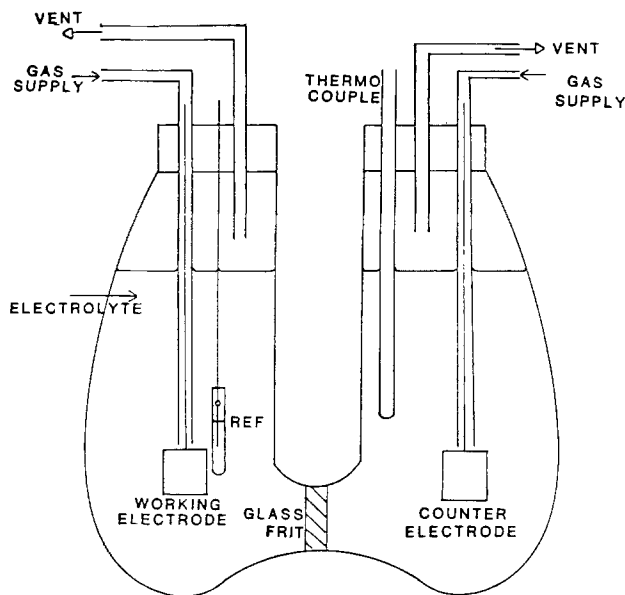


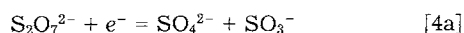
Fig. 2. Gas-tight cell for effluent analysis

solenoid relay connected to a Barber-Coleman no. 122-B temperature controller. Provisions were made for gas flow to and from the cells by means of 6.35 mm glass tubing. The gases were premixed primary-standard grades supplied by Matheson. The working electrode and counter-electrode were flat gold foils each of 8.3 cm² area. Mechanical support and electrical connection to the foils were provided by gold wires gold-soldered to the foils. The reference electrode was a silver wire dipping into a AgNO₃/KNO₃ melt contained in a sealed Pyrex capsule. A PAR 371 Potentiostat/Galvanostat with a Model 178 electrometer probe was used in most experiments to control the overall cell potential, the potential of either electrode with respect to the reference electrode, or the cell current. For studies of transient cell behavior, a Hewlett-Packard (HP) Model 3310B function generator was utilized. In some experiments a PAR 273 potentiostat, with automatic IR compensation, was employed. Gas analysis was by gas chromatograph (HP 5840) using both thermal conductivity and flame photometric detectors for sulfur dioxide.

Results

Effluent analysis.—Insight into the reactions taking place at the cathode may be gained by analyzing the effluent from the gas-tight cell. Nitrogen containing sulfur dioxide and oxygen at levels representative of the flue gas flows to the cathode, and the exit sulfur oxide concentration is monitored as a function of electrolyte composition and applied current.

Figure 3 shows the cathode-effluent sulfur oxide concentration (compared to open-circuit values) in a pure potassium pyrosulfate melt. The inlet gas contains 3000 ppm sulfur dioxide, 3% oxygen, and the balance nitrogen. The trend is clear; increasing the current leads to increased sulfur dioxide evolution. This is in agreement with work by Fang and Rapp (11a) who propose a cathodic reaction scheme resulting in sulfur dioxide production. Although their study utilized a sulfate melt at 900°C, pyrosulfate was identified as the active species. They did not analyze their reaction products but, based on cyclic voltammetry and chronopotentiometry, concluded that the pyrosulfate was reduced in a one-electron charge transfer reaction



with the sulfur dioxide produced in subsequent reactions.

In an atmosphere of pure sulfur dioxide, Durand *et al.* (11b) similarly deduced the following overall reduction in pyrosulfate

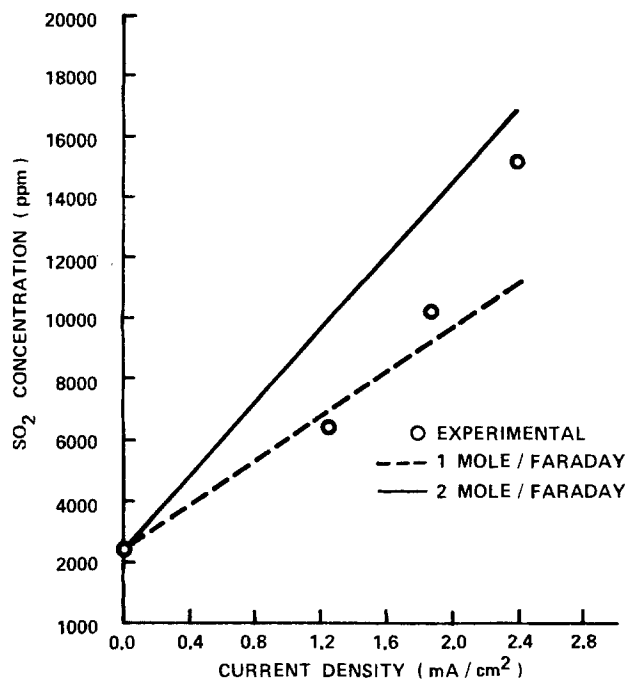
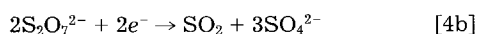
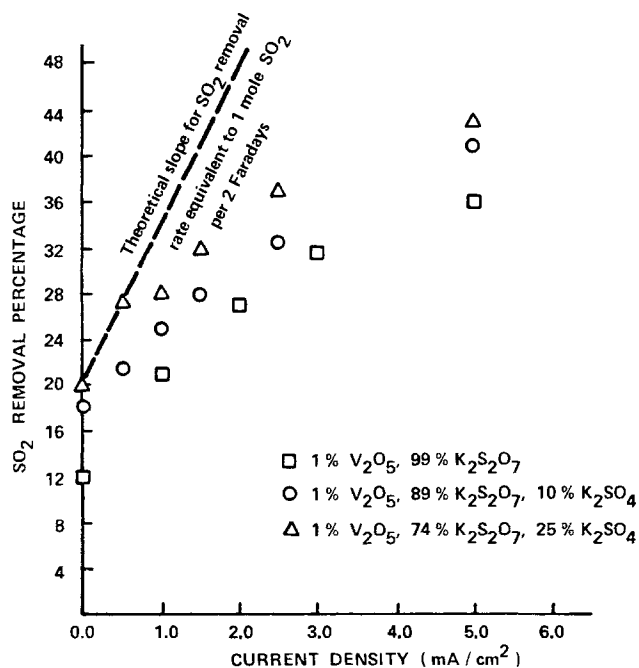
Fig. 3. Effluent sulfur dioxide concentration in pure K₂S₂O₇

Figure 3 also shows dashed lines comparing theoretical sulfur dioxide generation at 1 mol/Faraday and 2 mol/Faraday. The data at low current density correspond most closely with a production of 1 mol of sulfur dioxide per Faraday, while at higher current density they correspond more closely with 2 mol/Faraday. Some possible reaction schemes are presented later. The effect of K₂SO₄ and V₂O₅ addition is shown in Fig. 4. The inlet gas for these runs was 3000 ppm sulfur dioxide, 3% oxygen, 15% carbon dioxide, and the balance nitrogen. The data show exit sulfur dioxide concentrations relative to the inlet gas concentration.

With V₂O₅ addition, the most interesting results occur in melts containing 1% V₂O₅. Here, increasing the current reduces the cathode exit sulfur oxide concentration. Figure 4 shows that addition of SO₄²⁻ further enhances sulfur dioxide removal. With a 1% V₂O₅/25% K₂SO₄/74% K₂S₂O₇

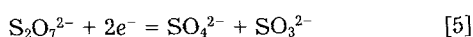
Fig. 4. Sulfur dioxide removal in K₂S₂O₇ melts containing V₂O₅ and K₂SO₄.

melt, up to 42% sulfur dioxide removal compared to open circuit is observed.

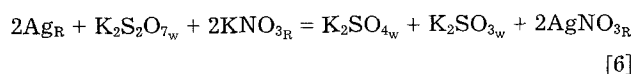
Thin film experiments.—Polarization data were taken for a system consisting of planar gold electrodes covered by a molten pyrosulfate film of variable thickness (1–3 mm) exposed to an atmosphere of variable gas composition. The limiting current was determined for each set of conditions. The results showed that the limiting current density, 7.0 mA/cm², was independent of the gas environment, suggesting that the predominant electrode reactions involve direct oxidation and reduction of species originally in the liquid phase.

Similar experiments by Shores and Fang (12) with a Na₂SO₄ melt showed a marked effect of gas composition on the limiting current. This led to the conclusion that the active species was supplied by the gas phase. Shores and Fang eliminated a number of reduction reaction possibilities by showing that an unreasonable value of the diffusion coefficient, *D* (calculated by assuming a stagnant film: $D = i_l \delta / nFC$), would be required for the experimental data to be consistent. In the present work, certain reduction reactions can also be eliminated in this manner. The concentration of any species other than pyrosulfate is found to be too low to give reasonable values of the diffusion coefficient.

Equilibrium potentials.—The equilibrium potential was measured for three melts under continuous bubbling of a gas consisting of 0.3% sulfur dioxide, 3.0% oxygen, and the balance nitrogen. Our data, Table I, show a significant dependence on the composition of the melt. The only reaction that predicts similar equilibrium potentials to our experimental data is



The overall reaction determining the equilibrium working (w) vs. reference (R) potential would then be



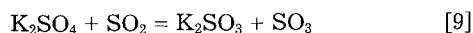
Therefore, the potential of the working with respect to the reference is given by

$$E_e = E^\circ - \frac{RT}{2F} \ln \frac{a_{\text{K}_2\text{SO}_{4w}} a_{\text{K}_2\text{SO}_{3w}} a_{\text{AgNO}_{3R}}^2}{a_{\text{Ag}_R}^2 a_{\text{K}_2\text{S}_2\text{O}_7} a_{\text{KNO}_{3R}}^2} \quad [7]$$

The standard potential and Nernst term may be calculated from thermodynamic data (13), approximating the activity of each species with its concentration. The concentrations of AgNO_{3R}, Ag_R, K₂S₂O_{7w}, and KNO_{3R} are known. The concentration of K₂SO_{4w} in the melt without added sulfate may be determined by considering the equilibrium



and that of K₂SO_{3w} from



However, with oxygen present, some of the sulfite is oxidized



As is well known, this oxidation is quite sluggish in the absence of a promoter such as V₂O₅ (14). Experimental and calculated results, shown in Table I, indicate that the oxidation is about 10% complete. The effect of increasing sulfate is, as expected from Eq. [7], to lower the equilibrium potential. Note that the concentration term accounts for about 1.5V.

Cyclic voltammetry performed on these melts as well as those containing V₂O₅, under a variety of gas compositions, corroborated and extended these results. These tests, being quite extensive, are reported elsewhere (15).

Chronoamperometry.—The current response to a low overpotential step at a planar electrode can be analyzed to obtain both diffusion and kinetic information under certain conditions (16): that the electrochemical reaction, even if multi-step, has only one rate-determining step; that the electrolyte is well supported; and that no strong specific adsorption is present on the electrode.

For these experiments the working, counter, and reference electrodes were immersed in molten K₂S₂O₇ at 340°C. The working electrode was subjected to cathodic potential steps of various magnitudes. The resulting current vs. time data were recorded on a storage oscilloscope.

The mathematical description of the relaxation of the current following a potential pulse has been presented by Nagy (16). If the total current is taken to be equal to the faradaic current after the initial rise of the potential (i.e., if the finite capacitive current flowing through the electrode at all times is ignored) the current can be given by

$$i = (W/t_2\lambda^2) \{ \exp(\lambda^2 t) \operatorname{erfc}(\lambda t^{1/2}) + 2\lambda(t/\pi)^{1/2} - \exp[\lambda^2(t - t_2)] \operatorname{erfc}[\lambda(t - t_2)^{1/2}] - 2\lambda[(t - t_2)/\pi]^{1/2} \} \text{ (for } t > t_2) \quad [11]$$

where

$$W = \frac{V}{R_s + R_r} \quad [12]$$

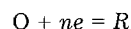
V is the applied potential step and *R_s* is the solution resistance and

$$R_r = \frac{\nu RT}{nF i_0} \quad [13]$$

ν is the number of working electrodes, *ν* is the stoichiometric number of the reaction mechanism, and *i₀* is the exchange current density.

$$\lambda = \frac{i_0}{\nu n F} \cdot \frac{R_s}{R_s + R_r} \left(\frac{1}{D_O^{1/2} C_O} + \frac{1}{D_O^{1/2} C_R} \right) \quad [14]$$

in the overall reaction



The resistance between the working and reference electrodes and the capacitance of the system were determined

Table I. Equilibrium potentials,^a *T* = 340°C

Initial electrolyte (mole percent)	<i>E_e</i> , vs. Ag/Ag ⁺ (V)	[K ₂ SO ₃] ^b calc.		
		Eq. [9] ^c	Eq. [10] ^c	Eq. [7] ^d
100% K ₂ S ₂ O ₇	0.700	1.7 × 10 ⁻²⁰	1.4 × 10 ⁻²³	2.0 × 10 ⁻²⁰
75% K ₂ S ₂ O ₇	0.550	7.0 × 10 ⁻¹⁶	2.4 × 10 ⁻²¹	2.4 × 10 ⁻²⁰
25% K ₂ SO ₄				
60% K ₂ S ₂ O ₇	0.520	2.2 × 10 ⁻¹⁵	3.9 × 10 ⁻²¹	3.8 × 10 ⁻²⁰
40% K ₂ SO ₄				

^a Gas phase: 0.3% SO₂, 3.0% O₂, bal. N₂.

^b *K₀* = 5.6 × 10⁻¹⁸.

^c *K₁₀* = 1.7 × 10⁻²¹.

^d *E⁰* = -0.915V.

^e *K₈* = 2.8 × 10⁻⁶.

to be about $1.5 \Omega\text{-cm}^2$ and $200 \mu\text{F}$, respectively. The resistance was measured with an ac bridge while the capacitance was estimated from current-step experiments. The characteristic times of the electrode system were evaluated as detailed by Nagy (16), allowing calculation of the time, t_2 , after which the errors introduced by using Eq. [11] will be less than 1%. For the present system, t_2 is less than 10 msec, and this figure was used as a convenient delay time before commencing current measurements.

The parameters W and λ were determined (by nonlinear computer regression) for cathodic potential steps of 25, 50, 75, 100, 150, 200, 250, and 300 mV. An example of a calculated curve and experimental data for a 50 mV step is shown in Fig. 5.

The exchange current density, i_0 , may be calculated by rearranging Eq. [12]. Table II summarizes the values of W and λ obtained from each cathodic potential step. It also shows the value of i_0 and $(1/D_O^{1/2}C_O + 1/D_R^{1/2}C_R)$ calculated from Eq. [12] and [14]. The results from these experiments were strikingly consistent over the wide range of overpotentials studied. They also are well within the applicability envelope illustrated by Nagy (16) for use of Eq. (11).

The average value of the cathodic exchange current density is about 0.030 A/cm^2 . This value is quite high, when compared with exchange currents found in molten carbonate [e.g., Ref. (17)], implying that the electrode reaction will not be limiting in a commercial device operating at 0.050 A/cm^2 with porous electrodes.

The average value of the diffusion parameter is $2.4 \times 10^7 \pm 0.8 \times 10^7 \text{ s}^{1/2} \text{ cm}^2/\text{mol}$. From the thin-film results presented earlier, the species being reduced is potassium pyrosulfate which is present at $C_O = 0.01 \text{ mol/cm}^3$. By substituting reasonable values for the diffusivities ($2 \times 10^{-5} \text{ cm}^2/\text{s}$), C_R can be estimated to be $0.9 \times 10^{-5} \text{ mol/cm}^3$. The concentration of sulfate ion in the bulk melt is calculated by considering reaction [8]. The equilibrium constant at 340°C is calculated from thermodynamic data to be 2.8×10^{-6} . If zero to 10% of the entering sulfur dioxide is oxidized to sulfur trioxide (as indicated from the results shown in Table I), the equilibrium concentration of K_2SO_4 is $(1.0\text{-}3.0) \times 10^{-5} \text{ mol/cm}^3$. This value is the same order of magnitude as that determined for C_R and indicates that pyrosulfate is being reduced to form sulfate in the overall reaction.

Discussion

In a melt of pure $\text{K}_2\text{S}_2\text{O}_7$, cathodic current causes evolution of sulfur dioxide in the range of 1-2 mol/Faraday. However, when K_2SO_4 is added to the melt, the equilibrium potential is affected, as shown in Table I. Added V_2O_5 brings about sulfur dioxide absorption under all cathodic currents. Sulfate addition further improves the sulfur dioxide removal.

Thin-film experiments showed conclusively that the gas phase was not directly involved in the electrochemical reaction, which is apparently a direct reduction of pyrosulfate

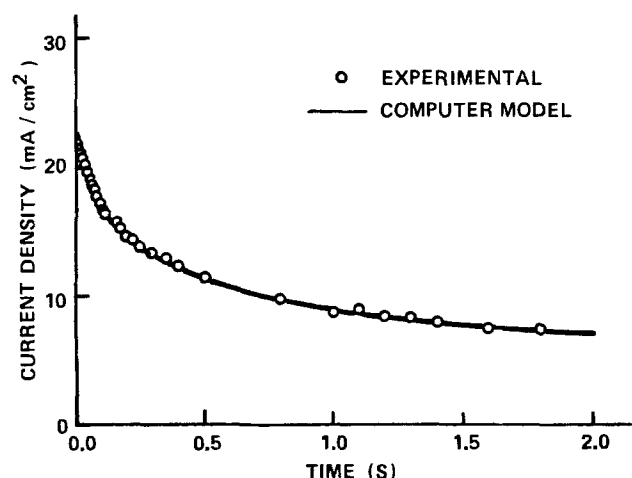


Fig. 5. Cathodic current decay after 50 mV potential step

Table II. Parameters obtained by fitting cathodic potential step data at 340°C

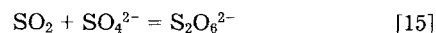
Potential step (V)	W (A/cm^2)	λ ($\text{s}^{-1/2}$)	i_0 (A/cm^2)	$\left(\frac{1}{D_O^{1/2}C_O} + \frac{1}{D_R^{1/2}C_R}\right)$ ($\text{s}^{1/2}\text{cm}^2\text{mol}^{-1}$)
0.025	0.0099	1.718	0.0264	3.09×10^7
0.050	0.0209	1.240	0.0300	2.23×10^7
0.075	0.0290	1.092	0.0249	1.96×10^7
0.100	0.0392	2.365	0.0262	4.25×10^7
0.150	0.0567	1.120	0.0236	2.01×10^7
0.200	0.081	1.093	0.0279	1.97×10^7
0.250	0.110	1.172	0.0349	2.11×10^7
0.300	0.139	1.074	0.0391	1.92×10^7

fate. Equilibrium potential measurements confirm the pyrosulfate-sulfate electrochemistry Eq. [5]. Further confirmation is seen in the consistency of the potential-step results. Thus, the evolution and/or SO_2 absorption takes place in subsequent (or preceding) chemical reaction.

The only scheme which can explain all these observations is one in which pyrosulfate is reduced electrochemically to intermediates which then decompose to evolve sulfur dioxide, but with added V_2O_5 and/or K_2SO_4 act to cause net absorption of sulfur dioxide.

The rate of sulfur dioxide evolution in pure $\text{K}_2\text{S}_2\text{O}_7$, as shown in Fig. 3, can only be explained by the one or two electron paths shown in Table III (Eq. [3-1a] and [3-1b]). The participation of superoxide (O_2^-) and peroxide (O_2^{2-}) has been observed in carbonate electrolytes (17) and in sulfates (18). Where diffusion allows, some sulfur dioxide either in the inlet or that generated, will react with these oxyanions, as in Eq. [3-2a] and [3-2b]. Either pathway, [3-1a] plus [3-2a] or [3-1b] plus [3-2b], yields the reduction reaction presumed by Durand *et al.* (11b), Eq. [4b]. Since their melt was saturated with 1 atm of sulfur dioxide at all times, no effect of changing sulfite concentration was seen.

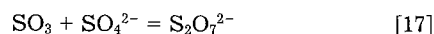
As cathodic overpotential is applied, there is apparently a slow shift in mechanism from Eq. [5] toward those which favor sulfur dioxide evolution, Eq. [3-1a] and [3-1b]. Added sulfate reduces the acidity of the melt and helps neutralize the sulfur dioxide, possibly through formation of dithionate



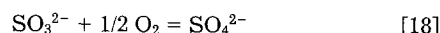
which can disproportionate to



with the sulfur trioxide quickly neutralized by any available sulfate



and the SO_3^{2-} partly oxidized by dissolved oxygen (in the form of superoxide or peroxide)



The addition of V_2O_5 promotes the oxidation, with the participation of the oxygen present in large excess, of sulfur dioxide to sulfur trioxide, although probably as dissolved, complex anions (e.g., Eq. [19])

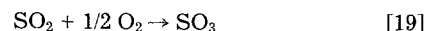


Table III. Reaction schemes

[3-1a]	$2\text{S}_2\text{O}_7^{2-} + e^- \rightarrow 2\text{SO}_2 + 2\text{SO}_4^{2-} + \text{O}_2^-$
[3-2a]	$\text{SO}_2 + \text{O}_2^- + e^- \rightarrow \text{SO}_4^{2-}$
[3-1b]	$2\text{S}_2\text{O}_7^{2-} + 2e^- \rightarrow 2\text{SO}_2 + 2\text{SO}_4^{2-} + \text{O}_2^{2-}$
[3-2b]	$\text{SO}_2 + \text{O}_2^{2-} \rightarrow \text{SO}_4^{2-}$
[3-3]	$2\text{SO}_2 + \text{O}_2 \xrightarrow{\text{V}_2\text{O}_5} 2\text{SO}_3$
[3-4]	$2\text{SO}_3 + 2\text{SO}_4^{2-} \rightarrow 2\text{S}_2\text{O}_7^{2-}$
Net:	$\text{SO}_2 + \text{O}_2 + 2e^- \rightarrow \text{SO}_4^{2-}$

The sulfur trioxide is again quickly neutralized by any available sulfate.

The net cathodic reaction, with V_2O_5 and excess sulfate in the melt is then given by Eq. [1] as seen in the higher temperature sulfate melt (5).

Reaction [1] indicates a sulfur dioxide removal rate dependence on current equivalent to 1 mol of sulfur dioxide per 2 Faradays of electrons. This theoretical slope is shown as the dashed line in Fig. 4. The experimental data show lower removal rates due to significant mass-transfer limitations. The liquid-phase mass-transfer coefficient, k_l , for the free-rise of a bubble of diameter d_p can be estimated by (20)

$$k_l = 0.42 \frac{D_1}{d_p} \left(\frac{\mu_1}{\rho_1 D_1} \right)^{1/2} \left(\frac{d_p^3 \rho_1 \Delta \rho g}{\mu_1^2} \right)^{1/3} \quad [20]$$

Along with the integrated expression for total removal (21)

$$N_{\text{final}} = N_{\text{init}} \exp \left(\frac{-6k_l t}{d_p} \right) \quad [21]$$

Using these equations with values of $D_1 = 2.0 \times 10^{-5}$ cm²/s (22), $\mu_1 = 0.1$ g cm/s (23), along with experimental values of $t = 0.5$ -1.0 s and $d_p = 0.3$ -0.6 cm, the mass-transfer limitation ranges from 16 to 51%, consistent with the experimental results. As shown in Fig. 4, the removal data parallel the reaction scheme prediction only at current densities well below the mass-transfer limit. Thus, at higher currents, the sulfate produced in the electrochemical step has insufficient opportunity to react with the gas. In a device with immobilized electrolyte in contact with gas-diffusion electrodes (Fig. 1) this limitation can be avoided.

At higher concentrations of sulfate ion at these temperatures, the generation of sulfur dioxide with current is substantially reduced. This is not unexpected because in pure sulfate melts at high temperature (600°C) the cathodic effluent has been shown (5) to contain significantly less sulfur dioxide than the inlet. The maximum concentration of sulfate that can be tested at 340°C is limited by its solubility.

Conclusions

The electrochemical reactions of sulfur dioxide and oxygen in a pyrosulfate-based melt have been studied. The experimental work focused on testing possible electrolytes for use in a flue gas desulfurization cell operating at a lower temperature than was previously possible (5).

In a two-compartment gas-tight cell, the analysis of the cathode effluent stream provided the most valuable information. In pure potassium pyrosulfate, sulfur dioxide was produced, eliminating pure $K_2S_2O_7$ as a candidate electrolyte. However, in 1% V_2O_5 -99% $K_2S_2O_7$, sulfur dioxide removal was seen, which increased with cathodic current. Addition of sulfate further enhanced the sulfur dioxide removal rate to a point suggesting possible commercialization for the process. A cathodic reaction scheme is pre-

sented; although tentative, it is consistent with our results and those of other workers.

Acknowledgments

The authors would like to thank the Pittsburgh Energy Technology Center of the Department of Energy for financial support.

Manuscript submitted Feb. 4, 1987; revised manuscript received July 30, 1987.

Georgia Institute of Technology assisted in meeting the publication costs of this article.

REFERENCES

1. S. H. Langer and R. G. Haldeman, *J. Phys. Chem.*, **68**, 962 (1964).
2. J. Winnick, R. D. Marshall, and F. H. Schubert, *Ind. Eng. Chem. Process. Des. Dev.*, **13**, 59 (1974).
3. M. P. Kang and J. Winnick, *J. Appl. Electrochem.*, **15**, 431 (1985).
4. J. Weaver and J. Winnick, *This Journal*, **130**, 20 (1983).
5. D. Townley and J. Winnick, *Ind. Eng. Chem., Process Des. Dev.*, **20**, 435 (1981).
6. P. J. Potter, "Power Plant Theory and Design," The Ronald Press Co., New York (1959).
7. A. Cheng and J. Winnick, *Electrochim. Acta*, **30**, 1631 (1985).
8. T. Kudo, H. Ohayashi, and M. Yoshida, *This Journal*, **124**, 321 (1977).
9. D. Townley and J. Winnick, *Electrochim. Acta*, **28**, 389 (1983).
10. D. Townley, Ph.D. Thesis, Georgia Institute of Technology (1981).
11. (a) W. C. Fang and R. A. Rapp, *This Journal*, **130**, 2335 (1983). (b) A. Durand, G. Picard, and J. Vedel, *J. Electroanal. Chem.*, **70**, 55 (1976).
12. D. A. Shores and W. C. Fang, *This Journal*, **128**, 346 (1981).
13. I. Barin and D. Knacke, "Thermochemical Properties of Inorganic Substrates," Springer Verlag, Berlin (1973); H. Flood and N. Boye, *Z. El. Ch.*, **66**, 184 (1962); H. Flood and T. Forland, *Acta Chem. Scand.*, **1**, 781 (1947).
14. B. Davidson and G. Thodos, *AIChE J.*, **10**, 568 (1964).
15. M. Franke and J. Winnick, *J. Electroanal. Chem.*, **238**, 163 (1987).
16. Z. Nagy, *This Journal*, **129**, 1943 (1982); *Electrochim. Acta*, **25**, 575 (1980); *ibid.*, **29**, 917 (1984).
17. A. J. Appleby and S. B. Nicholson, *J. Electroanal. Chem.*, **83**, 309 (1977).
18. C. O. Park and R. A. Rapp, *This Journal*, **133**, 1636 (1986).
19. P. H. Calderbank, *Chem. Eng. Prog.*, **49**, 585 (1983).
20. P. H. Calderbank and M. B. Moo-Young, *Chem. Eng. Sci.*, **16**, 39 (1961).
21. K. Scott, Ph.D. Thesis, Georgia Institute of Technology (1985).
22. E. Sundheim, "Fused Salts," McGraw-Hill Book Co., New York (1964).
23. G. Janz, "Molten Salt Handbook," Academic Press, New York (1967).